arXiv:1401.4014v1 [math.AP] 16 Jan 2014

Cancellation of Singularities in SAR for Curved Flight Paths and Non-Flat Topography

Andrew Homan

Abstract

We consider a mathematical model of synthetic aperture radar (SAR) with a known, possibly non-flat, topography. In this context we consider the problem of recovering the wavefront set of the ground reflectivity, given radar data measured along a curved flight path. We show that if singularities are located at "mirror points," then the resulting data may be smooth; in effect, the singularities "cancel." With a flat topography, these mirror points are always discrete, but we show that in a non-flat topography there may be infinite families of mirror points.

1 Introduction

Synthetic aperture radar (SAR) is a radar imaging technique using an airplane or satellite flying along a known flight path to illuminate the Earth (or another planet) with radar, while at the same time measuring the backscattered signal. From this data, one would like to image the electromagnetic reflectivity of the ground. We refer the reader to [7] and references therein for a practical introduction to SAR. It has been adapted for many applications, including imaging through the forest canopy [8, 9, 23], imaging ocean waves [11, 22], and more recently for material identification [2].

When the same antenna is used to produce the incident wave and measure the scattered wave, the configuration is referred to as monostatic SAR, which is the object of our study. Under an assumption that the surface being imaged is approximately flat, the forward operator mapping scene to data can be modelled as a restricted circular Radon transform [15, 21]. This operator has been studied in the context of integral geometry [4, 5, 1] and also as a model of thermoacoustic tomography [14, 13, 18].

A related SAR configuration requires two antennas, one emitting and one receiving, which follow distinct flight paths. This is called bistatic SAR, and there has been some study of the restricted elliptical Radon transform as a model for it [17, 10]. It can also be used to model the artifacts occuring in monostatic SAR in the presence of a reflecting wall [3]. While we do not study bistatic SAR here, these works are notable for their use of microlocal analysis and the interpretation of the forward operator as a Fourier integral operator. This is similar to our approach here.

The problem of object determination in SAR lends itself naturally to microlocal analysis. For applications in target identification, it is often only necessary to recover the outline of the object, which tends to present itself as a jump discontinuity in the reconstruction [6]. Under the flat surface approximation, Nolan and Cheney showed the forward operator is a Fourier integeral operator [20]. In [19], they also give an example of SAR with non-flat topography and mention some of its limitations. In this paper we elaborate on these limitations, particularly in the case of non-flat topography.

Even in a flat model of SAR, artifacts can appear. These artifacts are explained by the fact that the canonical relation is two-to-one in a neighborhood of the image of these artifacts. If, in addition, the flight path is straight and at a constant altitude, there is a well-known left-right ambiguity that obstructs the unique reconstruction of the scene on both sides of the flight path. Previously, using the restricted circular Radon transform as a model, Stefanov and Uhlmann showed that this left-right ambiguity persists in a microlocal sense when the flight path is curved [21].

Their analysis is built upon a notion of "mirror points" which characterize the artifacts in a way that is determined only by the geometry of the surface and the flight path. They show that the artifacts that appear at one mirror point are unitary images of the real signal under a microlocal Fourier integral operator. In this way each pair of mirror points induces an infinite family of singular reflectivity functions whose image under the forward operator is smooth. This phenomena, called "cancellation of singularities," presents an obstruction to any unique and stable reconstruction of the scene.

Our main goal is to characterize the artifacts in SAR with an arbitrary topography and arbitrary flight path. This requires analyzing the forward operator as a Fourier integral operator, which we do in the second section. Examining its canonical relation leads us to a generalization of the notion of a mirror points. In contrast to the case of flat topography, we find that an infinite number of mirror points may be related to a single observed singularity. Finally, we show cancellation of singularities for pairs of isolated mirror points, and present an example showing cancellation of singularities for an infinite family of mirror points.

2 Preliminaries

2.1 Model

In this section, we summarize the standard model of SAR [19, 20]. Each component of the electromagnetic field satisfies the wave equation $\partial_t^2 u - c^2 \Delta u = 0$. We assume the following data are known:

1. The flight path of the aircraft, given by a smooth, embedded curve γ parameterized with unit speed.

2. The surface of the Earth, Ψ, given by a smooth, embedded surface ψ.

We will use s to parameterize the flight path, and use (u, v) to locally parameterize Ψ. Let c be the speed of electromagnetic propagation; it is commonly assumed that c is the speed of light in air c_0 except for a singular perturbation supported on Ψ of the form:

$$c_0^{-2} - c^{-2} = V(u, v)\delta(\psi(u, v) - (x, y, z)).$$

Here, c_0 is the constant background speed of propagation and V is the ground reflectivity function, which we seek to recover from the electromagnetic field measured on the antenna as it travels along the flight path. We will assume that data is recorded over a finite interval $\mathcal{Y} = (s_1, s_2) \times (t_1, t_2)$. Under some assumptions on the geometry of the antenna, [19] finds the map from V to the recorded data is of the form,

$$FV(s, t) = \int_{\mathbb{R}\times\mathcal{X}} A(u, v, s, t, \omega)e^{-i\omega\left(t-\frac{2}{c_0}|\psi(u,v)-\gamma(s)|\right)}V(u, v)\, du\, dv\, d\omega,$$

where A is an amplitude of order two. By finite speed of propagation, the amplitude A is zero outside the "visible" set

$$\mathcal{X} = \left\{(u, v) : \exists s \in (s_1, s_2), \frac{2}{c_0}|\psi(u, v) - \gamma(s)| \in (t_1, t_2)\right\}.$$

In particular, this implies that A has proper support.

In what follows we will assume that the wavefront set of V is contained in $T^*\mathcal{X} \setminus 0$, i.e., $V \in C^\infty(\Psi \setminus \overline{\mathcal{X}})$. This is not to imply that all singularities in $T^*\mathcal{X} \setminus 0$ are recoverable from FV; only that "invisible" ones cannot be.

In order to recover V from FV, our goal will be to determine the circumstances under which F is a Fourier integral operator, and in those cases apply microlocal techniques to recover the wavefront set of V uniquely. In some cases, the geometry of Ψ and γ prevent the unique recovery of singularities, and we provide for all choices of Ψ and γ an infinite family of counterexamples V with nonempty wavefront set whose image, FV, is smooth – therefore, the singularities of V cannot be recovered.

We conclude this section with some convenient notation for the geometry of the flight path, adopted from [20].

Notation. *We will write $R(u, v, s) = \psi(u, v) - \gamma(s)$. Then the time required for a signal to leave $\gamma(s)$, reflect off $\psi(u, v)$, and return is $2|R(u, v, s)|/c_0$. The reflection off $\psi(u, v)$ propagates in the direction $\hat{R}(u, v, s) = R(u, v, s)/|R(u, v, s)|$.*

In what follows, we often use the notation shown in Figure 1. Let the projection of the vector $\hat{R}(u, v, s)$ onto the tangent plane of Ψ at (u, v) be $\pi_{T\Psi}\hat{R}(u, v, s)$.

2.2 Microlocal analysis of the forward operator

The model described in the previous section takes the forward operator to be an oscillating integral with phase

$$\phi(s, t, u, v, \omega) = \omega\left(t - \frac{2}{c_0}|R(u, v, s)|\right).$$

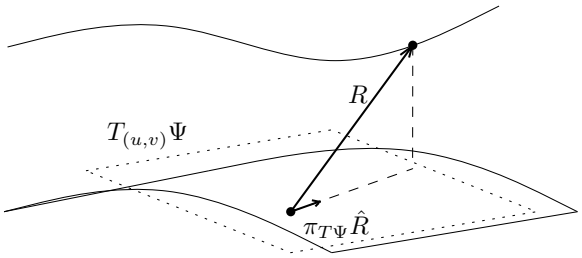

Figure 1: Notation for geometry of flight path and topography.

We take (s,t,σ,τ) as local coordinates on $T^*\mathcal{Y}$ and (u,v,ξ,η) as local coordinates on $T^*\mathcal{X}$.

Proposition 1. *If* $\operatorname{dist}(\Psi,\gamma)>0$*, then* F *is a Fourier integral operator associated to the Lagrangian submanifold*

$$\Lambda=\left\{(s,t,\sigma,\tau;u,v,\xi,\eta):\quad t=\frac{2}{c_0}|R(u,v,s)|,\right.$$
$$\sigma=\frac{2\tau}{c_0}\hat{R}(u,v,s)\cdot\dot{\gamma}(s),$$
$$\left.(\xi,\eta)=-\frac{2\tau}{c_0}\pi_{T\Psi}\hat{R}(u,v,s)\right\}.$$

Proof. The critical points of the phase function (with respect to ω) lie on the set

$$C=\left\{t=\frac{2}{c_0}|R(u,v,s)|\right\}.$$

The function $t-2|R(u,v,s)|/c_0$ is smooth away from the set $\{|R(u,v,s)|=0\}$. By our assumption that the flight path is separated from the surface of the Earth, this poses no problem. By the inverse theorem, C is a submanifold of $\mathcal{Y}\times\mathcal{X}\times(\mathbb{R}\setminus 0)$. Define Λ to be the image of C under the map:

$$(s,t,u,v,\omega)\mapsto(s,t,\partial_s\phi,\partial_t\phi,u,v,\partial_u\phi,\partial_v\phi).$$

By [12, Lemma 2.3.2], this is an immersed Lagrangian submanifold of $(T^*\mathcal{Y}\times T^*\mathcal{X})\setminus 0$ with respect to $\omega_{\mathcal{Y}}\oplus\omega_{\mathcal{X}}$, where $\omega_{\mathcal{X}}$ and $\omega_{\mathcal{Y}}$ are the canonical symplectic forms on $T^*\mathcal{X}\setminus 0$ and $T^*\mathcal{Y}\setminus 0$, respectively. □

The canonical relation Λ' of F is found by multiplying the last two coordinates (ξ,η) by -1. Recall that if $V\in\mathcal{E}'(X)$, then

$$\mathrm{WF}(FV)\subset\{q\in T^*\mathcal{Y}\setminus 0:(p,q)\in\Lambda',p\in\mathrm{WF}(V)\}.$$

As the data we can measure is confined to a finite interval $(s_1,s_2),(t_1,t_2)$, the source of any singularity in the data is confined to a subset of $T^*\mathcal{X}\setminus 0$

whose projection to $\mathcal{X}$ is bounded. To see this, note that the canonical relation requires the travel-time from the source of the signal to the plane to be bounded by t_2. This also can be seen from finite speed of propagation.

2.3 Sets on which Λ' is locally of graph type

Interpreting the forward operator F as a Fourier integral operator allows us to exploit the geometry of its canonical relation. In particular, there are some microlocalizations of F that are elliptic in the sense of [16, Def 25.3.4]; that is, their canonical relation is the graph of a symplectomorphism and their amplitude (relative to the phase ϕ in the usual representation) is nonzero in a neighborhood of their micro-support.

Here we determine the largest set on which Λ' is locally of graph type, with a view toward constructing microlocal parametrices of F later. At this point we distinguish between a canonical relation which is the graph of a diffeomorphism and a canonical relation which is the graph of a bijective diffeomorphism. However, there is no distinction locally, as we can always restrict to a yet smaller neighborhood on which the diffeomorphism is bijective.

Proposition 2. *Λ' is a homogeneous canonical relation that is locally of graph type away from the degenerate set $\Sigma = \Sigma_1 \cup \Sigma_2$, where*

$$\Sigma_1 = \left\{ (s,t,\sigma,\tau,u,v,\xi,\eta) : \pi_{T\Psi}\hat{R}(u,v,s) \parallel \nabla_{u,v}(\hat{R}(u,v,s)\cdot\dot{\gamma}(s)) \right\} \cap \Lambda',$$

and

$$\Sigma_2 = \left\{ (s,t,\sigma,\tau,u,v,\xi,\eta) : \pi_{T\Psi}\hat{R}(u,v,s) \parallel \partial_s \pi_{T\Psi}\hat{R}(u,v,s) \right\} \cap \Lambda'.$$

Proof. Let $\pi_L : \Lambda' \to T^*\mathcal{Y}\backslash 0$ and $\pi_R : \Lambda' \to T^*\mathcal{X}\backslash 0$ be the canonical projections of $T^*(\mathcal{Y}\times\mathcal{X}) \setminus 0$ onto its factors. We will show that Λ' is locally of graph type away from Σ by showing that $\nabla\pi_L$ is not of full rank only on Σ_1 and $\nabla\pi_R$ is not of full rank only on Σ_2.

We have the coordinate representation

$$\pi_L(s,\tau,u,v) = \left(s, \frac{2}{c_0}|R(u,v,s)|, \frac{2}{c_0}\tau\hat{R}(u,v,s)\cdot\dot{\gamma}(s), \tau \right)$$

from which we can calculate

$$\nabla\pi_L = \begin{bmatrix} 1 & 0 & 0 & 0 \\ * & 0 & \frac{2}{c_0}\pi_1\pi_{T\Psi}\hat{R}(u,v,s) & \frac{2}{c_0}\pi_2\pi_{T\Psi}\hat{R}(u,v,s) \\ * & * & \partial_u(\frac{2\tau}{c_0}\hat{R}(u,v,s)\cdot\dot{\gamma}(s)) & \partial_v(\frac{2\tau}{c_0}\hat{R}(u,v,s)\cdot\dot{\gamma}(s)) \\ 0 & 1 & 0 & 0 \end{bmatrix}$$

Here π_1, π_2 are the natural projections onto the first and second component of $\pi_{T\psi}\hat{R}(u,v,s)$.

As for π_R, we have that

$$\pi_R(s,\tau,u,v) = \left(u, v, \pi_1 \frac{2\tau}{c_0}\pi_{T\Psi}\hat{R}(u,v,s), \pi_2 \frac{2\tau}{c_0}\pi_{T\Psi}\hat{R}(u,v,s)\right)$$

Therefore,

$$\nabla\pi_R = \begin{bmatrix} 0 & 0 & \frac{2\tau}{c_0}\pi_1\partial_s\pi_{T\Psi}\hat{R}(u,v,s) & \frac{2\tau}{c_0}\pi_2\partial_s\pi_{T\Psi}\hat{R}(u,v,s) \\ 0 & 0 & \frac{2}{c_0}\pi_1\pi_{T\Psi}\hat{R}(u,v,s) & \frac{2}{c_0}\pi_2\pi_{T\Psi}\hat{R}(u,v,s) \\ 1 & 0 & * & * \\ 0 & 1 & * & * \end{bmatrix}$$

This has full rank, provided $(s,\tau,u,v) \notin \Sigma_2$. □

Remark. In a flat topography, linear flight path model of SAR, the degenerate set reduces to the set of covectors whose base points lie directly under the flight path. This is related to the well-known difficulty of imaging below the flight path in SAR.

If instead the flight path is curved, the degenerate set contains for each base point on the flight path a one-dimensional family of covectors. These covectors have the property that the line through them is tangent to the flight path at the base point. That the canonical relation of F is not of graph type near these covectors was shown in [20].

Finally, [19] mentions the difficulty of imaging points on a non-flat surface that are local minima of the travel-time function $2|R(u,v,s)|/c_0$. When (u,v,s) is such a point, $\hat{R}(u,v,s)\nabla\psi(u,v) = 0$, and so by the above analysis both left and right projections drop at least one rank.

The degenerate set $\Sigma \subset \Lambda'$ is then the complement of the largest open subset of Λ' which is locally of graph type. For any point $(p,q) \in \Lambda'$, there exists a small neighborhood that is not only of graph type, but is also such that it is the graph of a bijective diffeomorphism. These neighborhoods will play an essential role in constructing microlocal parametrices later on.

3 Mirror points

The most striking difference between SAR on a flat topography (with either curved or straight flight path) and SAR on a non-flat topography is the geometry of sets of mirror points. In the flat case each point in $T^*\mathcal{Y} \setminus 0$ is associated to at most two mirror points [20, 21]. In this section, we will show that such mirror point sets in SAR with non-flat topography may either not be discrete or may contain more than two mirror points.

Definition. *Fix $p \in T^*\mathcal{Y} \setminus 0$. Then the set of mirror points associated to p is the set*

$$M_p = \{q \in T^*\mathcal{X} \setminus 0 : (q,p) \in \Lambda'\} \subset T^*\mathcal{X} \setminus 0.$$

In other words, if we interpret Λ' as a (possibly multi-valued) function from $T^*\mathcal{X} \setminus 0$ to $T^*\mathcal{Y} \setminus 0$, M_p is the inverse image of p under Λ'.

In this paper, we consider only mirror points associated to the same covector along the flight path. However, there is a different, broader notion of mirror points discussed in [21], which are associated to more than one covector via a billard-like flow. In the non-flat case, the presence of possibly infinite families of mirror points makes this sort of global analysis more difficult. This is why we restrict ourselves to the microlocal notion of mirror points associated to the same covector.

The following proposition shows that, away from a degenerate set, the microlocal analysis of mirror points on a non-flat topography is similar to that on a flat topography, insofar as non-degenerate mirror points are isolated. However, non-degenerate mirror points may also be mirror to an infinite family of degenerate mirror points – a phenomena which does not occur in the flat case. Further, in some cases, all singularities may be degenerate.

Proposition 3. *Fix $p \in T^*\mathcal{Y} \setminus 0$. Let Σ_p be the set of points q such that $(p, q) \in \Sigma$, the degenerate set of the canonical relation. Let M_p be the set of mirror points associated to p. Then $M_p \setminus \Sigma_p$ consists of isolated covectors.*

Proof. By definition $\Sigma_p \subset M_p$. Recall Λ' is locally of graph type near $(p, q) \in \Lambda'$ for all $q \in M_p \setminus \Sigma_p$. Then, there are suitably small neighborhoods of each q such that Λ' acts as a bijective diffeomorphism on each neighborhood. Therefore, the non-degenerate mirror points are isolated. □

Remark. If the topography is flat and the flight path is straight, these non-degenerate mirror points appear to the left and right of the flight path, causing left-right ambiguity. If the flight path is curved, the non-degenerate mirror points again come in pairs, as studied in [21].

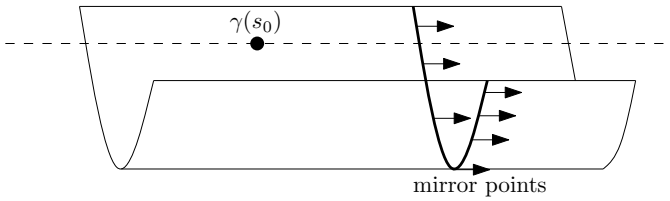

Figure 2: A cylindrical topography with flight path along the axis of rotation.

In Figure 2, we show an example of a cylindrical topography, which was also considered in [19]. Let $t > 2r/c_0$, where r is the radius of the cylinder. Associated to every covector over (s_0, t_0) is an infinite family covectors, with direction parallel to the axis of the cylinder. Similar examples with polygonal cross-sections (whose corners have been suitably rounded) can be constructed to yield any number of mirror points associated to the same covector.

4 Cancellation of singularities

In this section, we consider when signals in the data which would otherwise be observed in the data cancel each other out, in the manner of destructive interference. We show that for every pair of non-degenerate mirror points, there exists an infinite-dimensional family of ground reflectivity functions V whose image under the forward operator F is smooth. In other words, the microlocal kernel of F is infinite-dimensional, which obstructs a stable reconstruction.

Recall that for a fixed $p \in T^*\mathcal{Y} \setminus 0$, the set of mirror points associated with p are denoted M_p. The first results of this section concern the case where M_p contains at least two distinct, isolated mirror points, echoing the situation of SAR with flat topography.

4.1 Non-degenerate mirror points

Fix $p \in T^*\mathcal{Y} \setminus 0$. In this section, we consider the case when two isolated mirror points are associated to p. In general, the number of isolated mirror points associated to p may be greater than two. This contrasts with the case of flat topography, which has at most two mirror points associated to any signal. Our result in this case generalizes [21, Theorem 2.1] to a different model of SAR taking into account non-flat topography, arbitrary flight paths, and generic incident waves.

Theorem 1. *Let $\Gamma \subset T^*\mathcal{Y} \setminus 0$ be a small, open conic neighborhood of p, and suppose there exist isolated mirror points $q_1, q_2 \in M_p$ associated to p. Assume the amplitude of the forward operator F is nonzero in a neighborhood of $(\pi_{\mathcal{X}}(q_1), \pi_{\mathcal{Y}}(p)) \times \mathbb{R} \setminus 0$ and $(\pi_{\mathcal{X}}(q_2), \pi_{\mathcal{Y}}(p)) \times \mathbb{R} \setminus 0$. Let $\Gamma_1, \Gamma_2 \subset T^*\mathcal{X} \setminus 0$ be small, open conic neighborhoods of q_1, q_2 respectively whose image under Λ' is Γ.*

Then for every $V_1 \in \mathcal{E}'(\mathcal{X})$ such that $\mathrm{WF}(V_1) \subset \Gamma_1$, there exists $V_2 \in \mathcal{E}'(\mathcal{X})$ with $\mathrm{WF}(V_2) \subset \Gamma_2$ related by a Fourier integral operator whose canonical relation is a diffeomorphism between Γ_1 and Γ_2 such that $\mathrm{WF}(F(V_1 + V_2)) \cap \Gamma = \emptyset$.

Proof. As q_1, q_2 are isolated, there is a conic neighborhood of both such that the restriction of Λ' to either is the graph of a function. After perhaps shrinking both neighborhoods and Γ, we can construct two conic neighborhoods Γ_1, Γ_2 of each covector respectively such that the restriction of Λ' to either set is the graph of a bijective diffeomorphism onto Γ.

Let $\chi_1, \chi_2 \in C^\infty(T^*\mathcal{X} \setminus 0)$ be two cut-off functions such that χ_i is supported on $\overline{\Gamma_i}$, nonzero on Γ_i, and homogeneous of degree zero in the fiber variables. We write the quantization $\chi_i(u, v, D_u, D_v)$ as P_i, which is a pseudodifferential operator of order zero. Similarly, let $\chi \in C^\infty(T^*\mathcal{Y} \setminus 0)$ be a cut-off function with the same properties on Γ, and write $\chi(s, t, D_s, D_t) = P$.

By construction, $F_i = PFP_i$ is a Fourier integral operator with canonical relation equal to that of Λ' restricted to $\Gamma_i \times \Gamma$. This canonical relation is the graph of a diffeomorphism, and moreover that diffeomorphism is bijective.

Further, the amplitude of F_i is nonzero. They are elliptic in the sense of [16, Def 25.3.4], so there exist two microlocal parametrices F_i^{-1}.

Given $V_1 \in \mathcal{E}'(\mathcal{X})$ with $\mathrm{WF}(V_1) \subset \Gamma_1$, the calculus of Fourier integral operators implies that $V_2 = -F_2^{-1}F_1V_1$ has $\mathrm{WF}(V_2) \subset \Gamma_2$. From here we can calculate,

$$F(V_1 + V_2) = FV_1 + -FF_2^{-1}F_1V_1$$

As the $\mathrm{WF}(F_2^{-1}F_1V_1) \subset \Gamma_2$, $-FF_2^{-1}F_1V_1 = -F_2F_2^{-1}F_1V_1$ modulo a smoothing operator applied to V_1, and similarly for FV_1.

$$\begin{aligned} F(V_1 + V_2) &= F_1V_1 - F_2F_2^{-1}F_1V_1 \pmod{C^\infty} \\ &= F_1V_1 - F_1V_1 \pmod{C^\infty} \\ &= 0 \pmod{C^\infty}. \end{aligned}$$

As we have applied a microlocal cut-off supported on Γ, this shows the wavefront set of $F(V_1 + V_2)$ does not intersect Γ. □

Each pair of isolated mirror points therefore induces an infinite-dimensional family of counter-examples microlocally supported near that pair. So, at best, any reconstruction of $\mathrm{WF}(V)$ from FV can only proceed up to sets of mirror points. This accounts for the artifacts seen in many forms of SAR.

In addition, this theorem can be extended to any subset of non-degenerate mirror points. Given $V_i \in \mathcal{E}'(X), i = 1, \ldots, n-1$ microlocally supported near a family $q_i, i = 1, \ldots, n$ of non-degenerate mirror points, the proof above shows that there is

$$V_n = -F_n^{-1} \sum_{i=1}^{n-1} F_iV_i$$

microlocally supported near q_n such that

$$\sum_{i=1}^{n} FV_i \in C^\infty.$$

This yields yet more counter-examples to stable reconstruction.

So far we have only considered mirror points associated to the same covector above the flight path. As mentioned earlier, there is also a notion of mirror points associated to multiple covectors, considered in the flat case by [21].

For example, let q_1, q_2 be associated to p_1, and q_2, q_3 be associated to p_2. If Theorem 1 holds for (q_1, q_2, p_1) and (q_2, q_3, p_2) separately, then one cancel the singularity of V_1, microlocally supported near q_1, with V_3, microlocally supported at q_3 where,

$$V_3 = -F_3^{-1}F_2F_2^{-1}F_1V_1.$$

A similar argument shows that $F(V_1 + V_3)$ is smooth.

4.2 Degenerate mirror points

Finally, we present an example showing that infinite families of mirror points also permit the cancellation of singularities. It is important to note that the proof of Theorem 1 depends crucially on the mirror points being non-degenerate – otherwise, we cannot pass to a microlocalization whose canonical relation is of graph type. For this, we return to the example shown in Figure 2.

Example. Let Ψ be the cylinder given by $\psi(u,v) = (\cos u, v, 1-\sin u)$, where $(u,v) \in (0,\pi)\times\mathbb{R}$, and $\gamma(s) = (0,s,1)$. Let $V = f(u)H(v)$ where $H(v) = \chi_{[0,\infty)}$ is the Heaviside function and $f(u) \in C^\infty((0,\pi))$. Assume $A = 1$ uniformly.

When $A = 1$, the forward operator reduces to the Fourier transform of a delta function.

$$\begin{aligned} FV(s,t) &= \int_{\mathbb{R}\times\Psi} e^{-i\omega\left(t-\frac{2}{c_0}\sqrt{(v-s)^2+1}\right)} f(u)H(v)\,du\,dv\,d\omega \\ &= \left\langle \delta\left(t - \frac{2}{c_0}\sqrt{(v-s)^2+1}\right), f(u)H(v)\right\rangle \\ &= \left\langle \delta\left(t - \frac{2}{c_0}\sqrt{(v-s)^2+1}\right), H(v)\right\rangle \int_0^\pi f(u)\,du. \end{aligned}$$

The map

$$w(v) = t - \frac{2}{c_0}\sqrt{(v-s)^2+1}$$

is two-to-one onto the interval $(-\infty, t-2/c_0)$. To calculate the pull-back, we divide the domain of w into two intervals, $(-\infty, s)$ and (s,∞). Then there are two inverses v_- and v_+ with range on each interval, respectively:

$$v_\pm(w) = s \pm \sqrt{\frac{c_0^2}{4}(w-t)^2 - 1}.$$

In either case, the derivative is non-zero on $(-\infty, t-2/c_0)$, and explicitly,

$$\left|\frac{dv_\pm}{dw}(w)\right| = \frac{c_0^2}{4}\frac{t-w}{\sqrt{c_0^2(t-w)^2/4-1}}.$$

Using this, we may calculate the pullback of $\delta(w)$ via $w(v)$. Let

$$\alpha(t) = \sqrt{c_0^2 t^2/4 - 1}.$$

Then:

$$\begin{aligned} \langle \delta(w(v)), H(v)\rangle &= \left\langle \delta(w), \left|\frac{dv_\pm}{dw}(w)\right| [H(v_-(w)) + H(v_+(w))]\right\rangle \\ &= \frac{c_0^2}{4}\frac{t}{\sqrt{c_0^2t^2/4-1}}[H(s+\alpha(t)) + H(s-\alpha(t))] \end{aligned}$$

So, the forward operator reduces to

$$FV(s,t) = \frac{c_0^2}{4} \frac{t[H(s+\alpha(t)) + H(s-\alpha(t))]}{\sqrt{c_0^2 t^2/4 - 1}} \int_0^\pi f(u)\, du,$$

which vanishes whenever the integral of f vanishes. There is a subspace of $C^\infty((0,\pi))$ for which this is true with infinite dimension. Since

$$\mathrm{WF}(f(u)H(v)) = (\{v = 0\} \times \{\xi = 0\}) \setminus 0$$

and $\mathrm{WF}(FV(f(u)H(v))) = \emptyset$, this shows that singularities on degenerate mirror points may also cancel.

References

[1] M. Agranovsky and P. Kuchment. Uniqueness of reconstruction and an inversion procedure for thermoacoustic and photoacoustic tomography with variable sound speed. *Inverse Problems*, 23:2089, 2007.

[2] R. Albanese and R. Medina. Materials identification synthetic aperture radar: progress toward a realized capability. *Inverse Problems*, 29:054001, 2013.

[3] G. Ambartsoumian, R. Felea, V. Krishnan, C. Nolan, and E. T. Quinto. A class of singular Fourier integral operators in synthetic aperture radar imaging. *J. Funct. Anal.*, 264:246–269, 2012.

[4] G. Ambartsoumian and P. Kuchment. On the injectivity of the circular radon transform. *Inverse Problems*, 21:473, 2005.

[5] G. Ambartsoumian and P. Kuchment. A range description for the planar circular Radon transform. *SIAM J. Math. Anal.*, 38:681–692, 2006.

[6] M. Cheney and B. Borden. Microlocal structure of inverse synthetic aperture radar data. *Inverse Problems*, 19:173, 2003.

[7] M. Cheney and B. Borden. *Fundamentals of Radar Imaging*. SIAM, 2009.

[8] M. Cheney and C. Nolan. Synthetic-aperture imaging through a dispersive layer. *Inverse Problems*, 20:507–532, 2004.

[9] S. R. Cloude, D. G. Corr, and M. L. Williams. Target detection beneath foliage using polarimetric synthetic aperture radar interferometry. *Waves in Random Media*, 14:S393–S414, 2004.

[10] J. D. Coker and A. H. Tewfik. Multistatic SAR image reconstruction based on an elliptical-geometry radon transform. In *International Waveform Diversity and Design Conference*, pages 204–208, June 2007.

[11] F. Collard, F. Ardhuin, and B. Chapron. Extraction of coastal ocean wave fields from SAR images. *IEEE Journal of Oceanic Engineering*, 30:526–533, 2005.

[12] J. J. Duistermaat. *Fourier integral operators*. Birkhäuser, 1996.

[13] D. Finch, S. K. Patch, and Rakesh. Determining a function from its mean values over a family of spheres. *SIAM J. Math. Anal.*, 35(5):1213–1240, 2004.

[14] M. Haltmeier, O. Scherzer, P. Burgholzer, R. Nuster, G. Paltauf, and N. Bellomo. Thermoacoustic tomography and the circular Radon transform: Exact inversion formula. *Math. Models Methods Appl. Sci.*, 17:635–655, 2007.

[15] H. Hellsten and L. Andersson. An inverse method for the processing of synthetic aperture radar data. *Inverse Problems*, 3:111–124, 1987.

[16] L. Hörmander. *The Analysis of Linear Partial Differential Operators IV: Fourier Integral Operators*. Springer, 1985.

[17] V. Krishnan and E. Quinto. Microlocal aspects of common offset synthetic aperture radar imaging. *Inverse Problems and Imaging*, 5:659–674, 2011.

[18] P. Kuchment and L. Kunyansky. Mathematics of thermoacoustic tomography. *Euro. J Appl. Math.*, 19:191–224, 2008.

[19] C. Nolan and M. Cheney. Synthetic aperture inversion for arbitrary flight paths and non-flat topography. *IEEE Trans. Image Process.*, 12:1035–1044, 2003.

[20] C. Nolan and M. Cheney. Microlocal analysis of synthetic aperture radar imaging. *J. Fourier Anal. Appl.*, 10:133–148, 2004.

[21] P. Stefanov and G. Uhlmann. Is a curved flight path in SAR better than a straight one? SIAM J. Appl. Math. 2013, to appear.

[22] C. Swift and L. R. Wilson. Synthetic aperture radar imaging of moving ocean waves. *IEEE Trans. Antennas and Propagation*, 27:725–729, 1979.

[23] T. Varslot, J. H. Morales, and M. Cheney. Synthetic-aperture radar imaging through dispersive media. *Inverse Problems*, 26:025008, 2010.